Conceptual Analysis for the Backscattering Spectrometer at the Spallation Neutron Source

K. W. Herwig
Oak Ridge National Laboratory
June 18, 1999
ES-1.1.8.4-6017-RE-A-00

Table of Contents

1. Executive Summary

This instrument is a near backscattering, crystal-analyzer spectrometer designed to provide high energy resolution with an extended range of momentum transfer. To some extent these are mutually exclusive requirements and this is reflected in an instrument design consisting of two separate hemispheres. The Si (111) crystal analyzers will provide extremely high energy resolution, 2.2 μeV, fwhm at the elastic peak, and a *Q*-range of 0.1 to 2.0 $Å^{-1}$. The Si (311) analyzer crystals will provide a more modest energy resolution of 10 μeV, fwhm, at the elastic peak with an extended *Q*-range of 0.6 to 3.8 $Å^{-1}$. The combination of high count rate, extended dynamic range in energy transfer, along with these resolution characteristics result in a spectrometer that will provide unprecedented opportunities for new science to the neutron scattering community.

1.1 Performance Capabilities

Table I lists the operating parameters of the instrument for near elastic scattering. The range of energy transfers, ω, was chosen symmetrically about the elastic peak. In practice the bandwidth, Δλ, can be shifted to correspond to a different range of ω. The instrument was designed to use the full operating frequency of the source, 60 Hz, giving Δλ = 0.785 Å. However, for some experiments an extended wavelength band is required. In this case the wavelength band using the Si (111) analyzers may be increased by eliminating intervening pulses using one of the bandwidth choppers as a pulse suppression chopper. By eliminating one pulse in two the wavelength band can be doubled. This feature is likely to be necessary when using the diffraction capabilities of the spectrometer where the experimenter might choose to use one pulse in 6 to obtain a Δλ of 4.5 Å. The wavelength band cannot be increased when using the Si (311) analyzers as this bandwidth is limited by order contamination from the analyzer crystals.

Table I. Spectrometer performance for near elastic scattering.

Analyzer Crystal	λ_f (Å)	Δλ (Å)	ω-range (μeV)	δω (fwhm) (μeV)	*Q*-range ($Å^{-1}$)	δ*Q* (fwhm) ($Å^{-1}$)
Si (111)	6.267	0.785	$-258 < \omega < 258$	2.2	0.1 – 2.0	0.1 – 0.05
Si (311)	3.273	0.117	$-279 < \omega < 279$	10	0.6 – 3.8	0.1 – 0.05

Table II lists the operating parameters of the instrument when used for inelastic scattering using the Si (111) analyzers operating at the source frequency. The *Q*-range and Δω are given for ω at the center of the accepted band of energy transfers. Note that this band of energy transfers can be extended using the chopper system to eliminate pulses. The maximum ω = 18 meV is obtained for incident neutron wavelengths of ~2 Å. Figure 1 shows the *Q*-ω band that can be reached using the Si (111) analyzers. The accessible range lies between the solid black lines and –1.5 meV < ω < 18 meV. The bandwidth can be shifted to any portion of this range of ω. The solid colored bands indicate what can be achieved when operating the instrument at 60 Hz. The blue band would correspond to a typical quasielastic measurement where the bandwidth is centered

at ω = 0 meV. The green band is centered about energy transfers of 5 meV and the red band was chosen to extend to the maximum energy transfer of ω = 18 meV.

Table II. Spectrometer performance for inelastic scattering using the Si (111) analyzers and operating at the source frequency of 60 Hz. The resolution quoted and *Q*-range are for the center of the ω-range.

ω (meV)	ω-range (meV)	Δω (fwhm) (μeV)	*Q*-range ($Å^{-1}$)
0	-0.258 < ω < 0.258	2.2	0.1 – 2.0
1.0	0.538 < ω < 1.464	2.8	0.2 – 2.2
2.0	1.30 < ω < 2.70	3.5	0.4 – 2.4
5.0	3.42 < ω < 6.59	5.8	0.9 – 2.8
10.0	6.55 < ω < 13.46	10.6	1.4 – 3.7

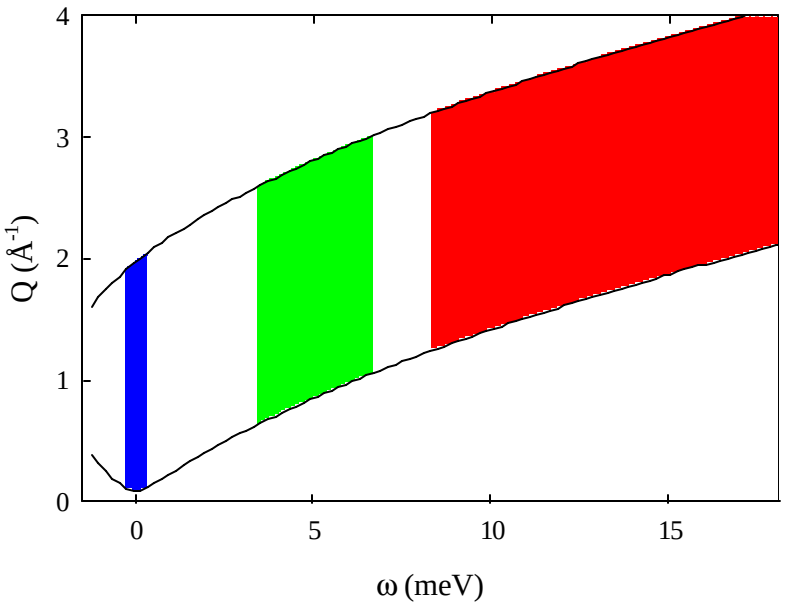

Figure 1. *Q*-ω band accessible to the spectrometer using the Si (111) analyzers. The accessible range lies between the solid black lines and extends from –1.5 meV < ω < 18 meV. The solid colored bands indicate operation of the instrument at 60 hz where the blue region has the available bandwidth centered at ω = 0, the central region is centered at ω = 5 meV, and the red band was selected to extend to ω = 18 meV , the maximum that can be reached.

It is also intended that some diffraction detectors be included for use in monitoring the state of the sample. Sufficient space remains in backscattering for a reasonably large detector of angular range ±20 deg. Detectors can also be placed above or below the analyzers at desired scattering angles. The performance of such a suite of diffraction detectors is yet to be determined. However, it is likely that they will only be useful when operating the spectrometer with an extended bandwidth provided by pulse elimination.

1.2 Instrument Description

Figure 2 shows a schematic view of the instrument and Table III lists the components and parameters of the instrument. Figures 3 and 4 show 3-d views of the instrument.

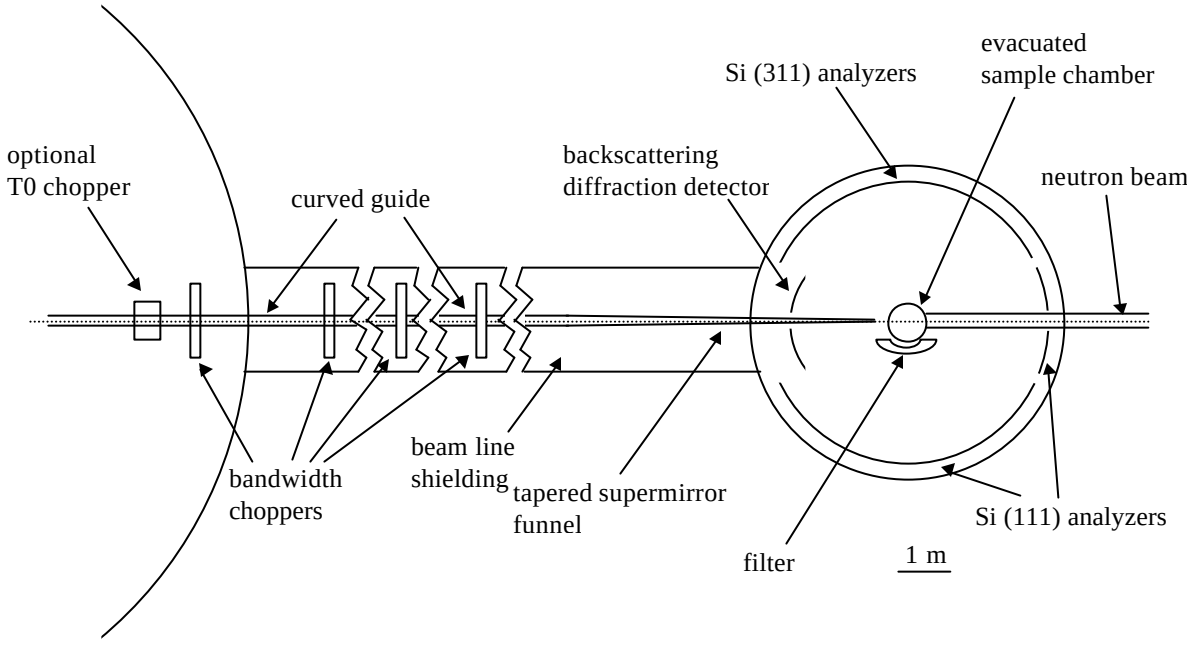

Figure 2. Schematic view of the spectrometer.

The analyzers from 20 deg to 160 deg in scattering angle are split in the horizontal plane containing the sample. Each segment of analyzer is focused onto a different detector bank. The top half of the analyzer is focused onto the top detector array and the lower half is focused onto the lower detector array. This split in the detector arrays is required in order to keep the Bragg angle and flight path uncertainties within acceptable ranges and still achieve a reasonable amount of angular coverage (±22 deg from the scattering plane). The forward analyzers cover as much solid angle as possible without blocking the adjacent analyzer segments. The parameters in this

document refer to this analyzer as composed entirely of Si (111) crystals. In principle, one half of this analyzer could be populated with Si (311) crystals, but it was thought that for low-*Q* inelastic scattering it would be better to populate both halves with Si (111) crystals.

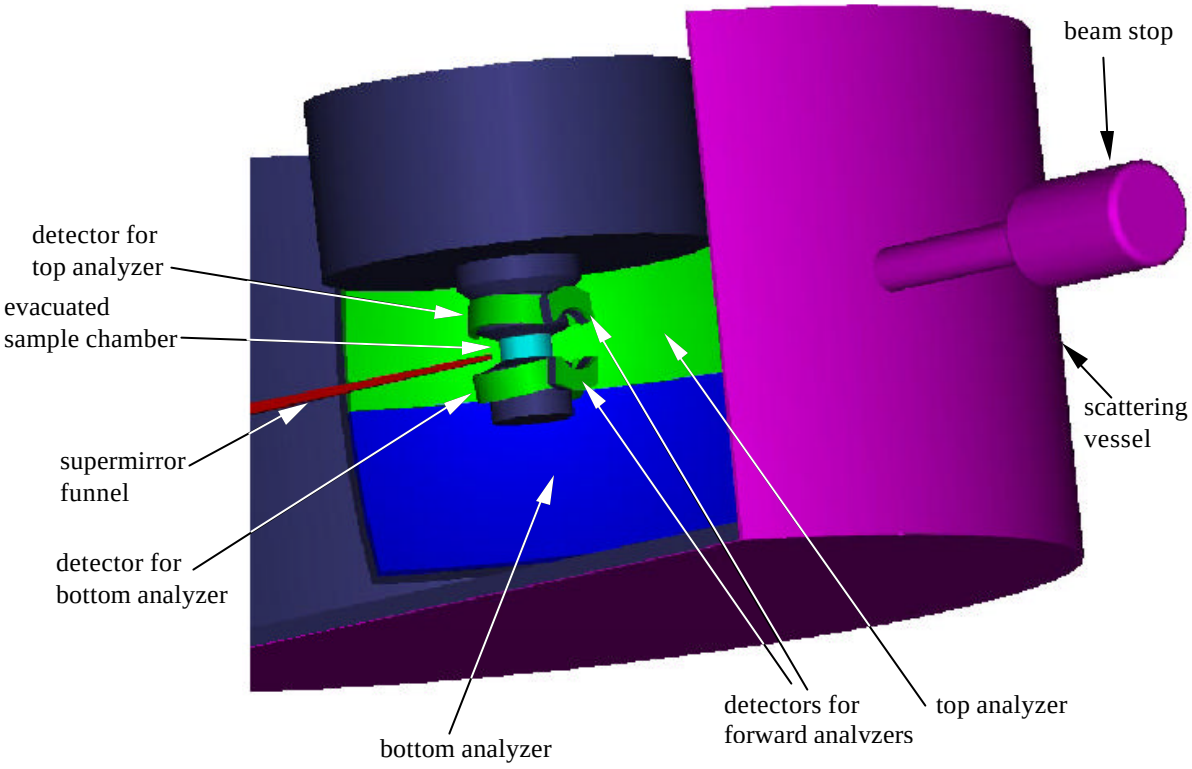

Figure 3. Three-dimensional rendered view of the spectrometer. Parts of the scattering chamber and one side of the analyzer system have been excluded for clarity. The two halves of the analyzer are colored differently for illustration, but would both be covered with Si (311) crystals. Detectors for the analyzers shown are obscured by the sample chamber.

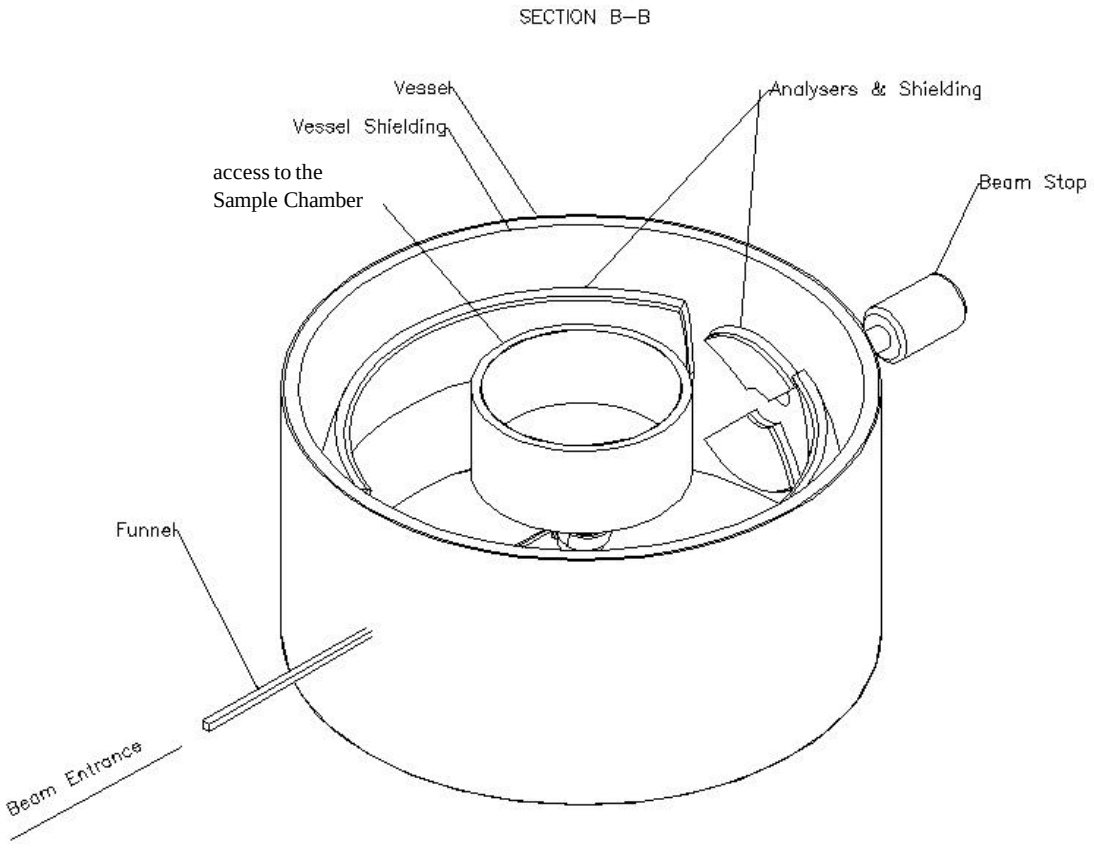

Figure 4. Three-dimensional line-drawing of the spectrometer from above.

Table III. Parameters for the Backscattering Spectrometer

.

Component	Parameter	Value
Source	Moderator	Liquid H2, centerline poisoned, decoupled
Geometry	Moderator-Sample Distance	84.0 m
	Sample-Analyzer Distance	2.50 m nominal
	Analyzer-Detector Distance	2.179 m nominal
	Total Final Flight Path	4.679 m ± 0.0035 m
T_0 Chopper (optional, based on guide performance)	Type	Horizontal-axis
	Radius to Beam Center	25 cm
	Length	30 cm
	Distance from Moderator	6.0 m
	Frequency	60 hz
	Beam width at chopper	10 cm

Bandwidth Chopper 1	Type	Disk
	Radius to Beam Center	25 cm
	Distance from Moderator	7.0 m
	Frequency	variable 10 to 60 hz
	Beam Width at Chopper	10 cm
	Wavelength Range to Open or Close	0.77 Å @ 60 hz
Bandwidth Chopper 2	Type	Disk
	Radius to Beam Center	25 cm
	Distance from Moderator	9.25 m
	Frequency	variable 10 to 60 hz
	Beam Width at Chopper	10 cm
	Wavelength Range to Open or Close	0.58 Å @ 60 hz
Bandwidth Chopper 3	Type	Disk
	Radius to Beam Center	25 cm
	Distance from Moderator	54.0 m
	Frequency	variable 10 to 60 hz
	Beam Width at Chopper	10 cm
	Wavelength Range to Open or Close	0.1 Å @ 60 hz
Bandwidth Chopper 4	Type	Disk
	Radius to Beam Center	75 cm
	Distance from Moderator	60.0 m
	Frequency	60 hz
	Beam Width at Chopper	10 cm
	Wavelength Range to Open or Close	0.025 Å
Guide	Type	curved
	Radius of Curvature	4.3 km
	Coating, top and sides	$2 \times \theta_c^{Ni}$ supermirror
	Channel Width	10 cm
	Channel Height	12 cm
	Moderator-Guide Distance	2.50 m
	Guide Length	76.2 m horizontal 75.2 m vertical
Guide Funnel	Coating, top and sides	$3 \times \theta_c^{Ni}$ supermirror
	Width at Exit	3 cm
	Height at Exit	3 cm
	Funnel Length	5 m horizontal 6 m vertical
	End of Funnel-Sample Distance	30 cm

Beamline Shielding	Steel radial thickness around beam	0.7 m
	Paraffin radial thickness around steel	0.2 m
	Channel for guide	0.3 m x 0.3 m
	Length	62 m (59 m to reach line of sight from moderator)
Beam Stop	Steel	1.6 m x 1.6 m x 2.6 m
	Paraffin radial thickness around steel	0.2 m
	Re-entrant hole in steel	0.2 m x 0.2 m x 0.5 m
Sample	Width	3.0 cm
	Height	3.0 cm
Analyzer Crystals	Side 1	Si (111)
	Bragg angle	88.0 deg
	Final neutron λ	6.267 Å
	Radius of Curvature	2.50 m
	Thickness	2 mm
	$\delta d/d$	3.5×10^{-4}
	Angular Coverage	$20 \text{ deg} < \theta < 160 \text{ deg}$
	Solid Angle Coverage	1.2 ster
	Analyzer Surface Area	7.5 m^2
	Filter	Cooled Be or BeO
	Side 2	Si (311)
	Bragg angle	88.0 deg
	Final neutron λ	3.273 Å
	Radius of Curvature	2.50 m
	Thickness	2.3 mm
	$\delta d/d$	4.0×10^{-4}
	Angular Coverage	$20 \text{ deg} < \theta < 160 \text{ deg}$
	Solid Angle Coverage	1.2 ster
	Analyzer Surface Area	7.5 m^2
	Filter	none
	Forward Scattering	Si (111)
	Bragg angle	88.0 deg
	Final neutron λ	6.267 Å
	Radius of Curvature	2.50 m
	Thickness	2 mm
	$\delta d/d$	3.5×10^{-4}
	Angular Coverage	$5 \text{ deg} < \theta < 20 \text{ deg}$
	Solid Angle Coverage	0.09 ster
	Analyzer Surface Area	0.6 m^2
	Filter	Cooled Be or BeO

Detectors	Side 1 Type	^{3}He proportional LPSD, 1 cm spatial resolution
	Array 1	1760 cm^2
	Diameter	1 cm
	Length	18 cm active length
	Number	~100 tubes
	Location	above scattering plane
	Array 2	1760 cm^2
	Diameter	1 cm
	Length	18 cm active length
	Number	~100 tubes
	Location	below scattering plane
	Side 2 Type	^{3}He proportional LPSD, 1 cm spatial resolution
	Array 1	1760 cm^2
	Diameter	1 cm
	Length	18 cm active length
	Number	~100 tubes
	Location	above scattering plane
	Array 2	1760 cm^2
	Diameter	1 cm
	Length	18 cm active length
	Number	~100 tubes
	Location	below scattering plane
	Forward Scattering Type	^{3}He proportional LPSD, 1 cm spatial resolution
	Array 1	740 cm^2
	Diameter	1 cm
	Length	18 cm active length
	Number	~40 tubes
	Location	above scattering plane
	Array 2	740 cm^2
	Diameter	1 cm
	Length	18 cm active length
	Number	~40 tubes
	Location	below scattering plane
	Backscattering Diffraction	To Be Determined

2. Instrument Design

The general philosophy followed in the design of this spectrometer was to focus initially on the design requirements for high energy resolution. Given the incident flight path dictated by this requirement, a secondary spectrometer was designed using shorter wavelength neutrons to extend the *Q*-range.

2.1 Resolution Function

The quantity of particular interest in this spectrometer is the resolution in energy transfer, ω,

$$\omega = E_i - E_f \qquad 2.1.1$$

where E_i is the incident neutron energy and E_f is the final neutron energy. On a crystal analyzer spectrometer, E_f is fixed by Bragg reflection from the analyzer crystals and the incident energy is determined by neutron time of flight as

$$E_i = \frac{5.2276 \text{ x } 10^{-6} L_i^2}{\left(t - t_f - t_0\right)^2} \qquad 2.1.2$$

where L_i is the moderator-sample distance, t is the total flight time as measured in a detector, t_f is the time for the neutron of known final energy to travel from the sample to analyzer to detector, and t_0 is the emission time of the neutron from the moderator. The constant is correct for E_i in meV, L_i in m, and time in sec. The final neutron energy is given by

$$E_f = \frac{81.787}{4d^2 \sin^2\left(\theta_B\right)} \qquad 2.1.3$$

where d is the d-spacing of the analyzer crystal and θ_B is the analyzer Bragg angle. Differentiating Eqn. 2.1.1 gives the uncertainty in the energy transfer

$$\delta\omega = 2E_i\left(\frac{\delta L_i}{L_i} + \frac{\delta t_0 + \delta t_f}{t - t_f - t_0}\right) + 2E_f\left(\frac{\delta d}{d} + \cot\left(\theta_B\right)\delta\theta_B\right) \qquad 2.1.4$$

The final neutron flight time is determined from

$$t_f = \frac{L_f \, 2d \sin\left(\theta_B\right)}{3955.4} \qquad 2.1.5$$

where L_f is the flight path length from the sample-analyzer-detector. Differentiating Eqn.

2.1.5 gives the uncertainty in the final flight time

$$\delta t_f = \frac{2}{3955.4}\left(\delta L_f\, d \sin(\theta_B) + \delta d L_f \sin(\theta_B) + \delta\theta_B L_f\, d \cos(\theta_B)\right) \quad 2.1.6$$

For this spectrometer design, the first term in Eqn. 2.1.6 is at least 3 times greater than the other terms and thus dominates the uncertainty in final flight time. The terms in Eqn. 2.1.4 can be separated into those dependent on the primary spectrometer (components before the sample) and the secondary spectrometer (components after and including the sample). Taking the approximation that the terms are independent and that the uncertainties add in quadrature yields

$$\delta\omega = \sqrt{\delta\omega_P^2 + \delta\omega_S^2} \quad 2.1.7$$

where the contribution of the primary spectrometer to the resolution is

$$\delta\omega_P = 2E_i \left(\left(\frac{\delta L_i}{L_i} \right)^2 + \left(\frac{\delta t_0}{t_i} \right)^2 \right)^{\frac{1}{2}} \quad 2.1.8$$

Typically, the first term in this equation is small compared to the second. The incident neutron flight time, t_i, is given in terms of the incident neutron wavelength, λ_i, as

$$\begin{aligned} t_i &= t - t_f - t_0 \\ &= \frac{L_i \lambda_i}{3955.4} \end{aligned} \quad 2.1.9$$

The contribution of the secondary spectrometer is

$$\delta\omega_S = 2\left(E_i^2 \left(\frac{\delta t_f}{t_i} \right)^2 + E_f^2 \left[(\cot(\theta_B)\delta\theta_B)^2 + \left(\frac{\delta d}{d} \right)^2 \right] \right)^{\frac{1}{2}} \quad 2.1.10$$

It is also important to understand the contributions to the *Q*-resolution particularly for energy transfers near the elastic peak. In this case, the momentum transfer is given by

$$Q = \frac{4\pi \sin\left(\frac{\theta}{2}\right)}{\lambda_f} \quad 2.1.11$$

where θ is the angle between the incident neutron beam and the scattered beam.

Differentiating Eqn. 2.1.11 gives the uncertainty in Q where $\delta\lambda_f$ is small as

$$\delta Q = \frac{4\pi}{\lambda_f}\cos\left(\frac{\theta}{2}\right)\frac{\delta\theta}{2} \qquad 2.1.12$$

The contributions to $\delta\theta$ can be taken as independent, adding in quadrature, so that

$$\delta Q = \frac{4\pi}{2\lambda_f}\cos\left(\frac{\theta}{2}\right)\sqrt{\delta\theta_i^2 + \delta\theta_S^2 + \delta\theta_A^2} \qquad 2.1.13$$

where the incident beam divergence, $\delta\theta_i$, is determined by the guide transmission. The sample dimension contribution has two terms, one for the vertical and one for the horizontal dimension, and is given by

$$\delta\theta_S = \sqrt{\left(\frac{H_S}{2L_f}\right)^2 + \left(\frac{W_S}{2L_f}\right)^2} \qquad 2.1.14$$

where H_S and W_S are respectively the height and width of the sample. The acceptance of the analyzer, $\delta\theta_A$, provides the final contribution to $\delta\theta$.

2.2 Resolution Contributions

Traditionally, the resolution contributions from the primary and secondary spectrometer are matched in an effort to optimize the count rate in the detectors for a given resolution. This is done under the assumption that neutron flux is lost evenly by both components as the resolution is improved. This is not so obvious when using a guide system for the primary spectrometer but it provides a reasonable starting point.

For many reasons, it is desirable to design this spectrometer with the analyzers operating slightly off backscattering. The detectors can then be placed on the same side of the sample as the analyzers and shielded from the sample, improving the operation of the instrument. The amount of solid angle available to the analyzers is effectively doubled as both sides of the spectrometer can be used (this flexibility has been used in this design to provide two modes of operation using the two different analyzer crystals). Detector placement becomes simpler as the design moves farther from backscattering but the second term in Eqn. 2.1.10 becomes more important. The design philosophy is to stay as close to backscattering as possible allowing for the detector placement. A reasonable choice is 2 deg off backscattering so that the Bragg angle is 88 deg.

As can be seen in Fig. 5, for a Bragg angle of 88 deg the second term in Eqn. 2.1.10 is ~0.75 μeV. A reasonable total energy resolution is then somewhere around 2 μeV (fwhm) implying a contribution from the primary spectrometer of ~1.4 μeV. Putting this requirement into Eqn. 2.1.8 yields an incident flight path of ~84 m, for a neutron λ of 6.267 Å and the supercritical hydrogen moderator. The other consideration on incident flight path is that one expects the highest backgrounds from the source to occur at times

when the protons are incident on the target, the prompt pulse. This moderator-sample path length results in the elastic peak from the Si (111) analyzers being midway in ω between successive pulses of the proton beam.

This moderator will be poisoned and decoupled, providing a polychromatic beam of cold neutrons to the instrument. For the current design, the moderator was taken as centerline poisoned which provides neutron pulse widths of

$$\delta t_0(\lambda) = \lambda \times 5.77 + 8.8\ (\mu\text{sec}) \qquad 2.2.1$$

for the wavelengths of use to this spectrometer. For λ = 6.267 Å (Si (111) analyzers) this corresponds to an emission time uncertainty of 45 μsec. A moderator poisoned more shallowly could provide a sharper pulse, resulting in a shorter instrument. However, moderator Intensity/δt_0^2 is approximately constant. If one chose a pulse width half as long giving a spectrometer half as long, the integrated flux from the moderator would go down a factor of 4. Having the instrument closer does not reduce this factor because the guide system already transports as much beam angular divergence as can be profitably used. The only gain is dynamic range (a factor of 2), which could also be achieved by using pulse elimination at a cost of a factor of 2 rather than a factor of 4 in flux. On the other hand the instrument could be made longer and gain in neutron flux, however, this costs dynamic range and would result in a guide system that is unwieldy.

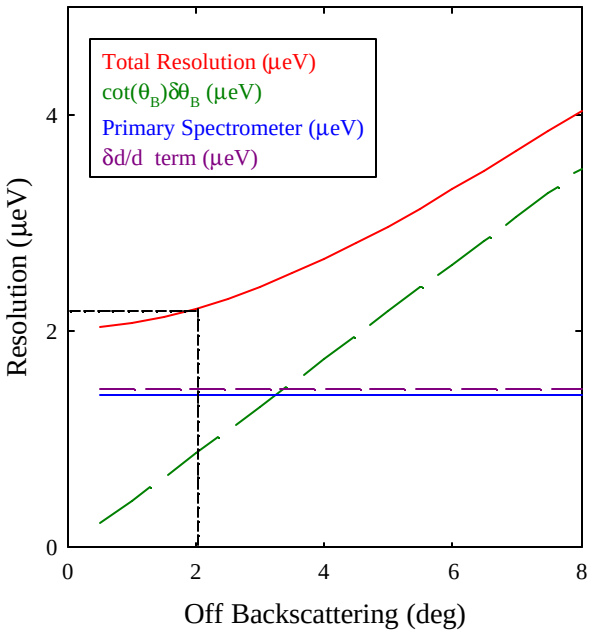

Figure 5. Resolution contributions of the spectrometer for the Si (111) analyzers at ω = 0. The horizontal axis is the difference between 90 deg and the Bragg angle. For completeness, the total resolution curve is plotted including all terms described in Eqns. 2.1.1 – 2.1.10. The light dashed curves illustrate the specified design condition. The solid horizontal line represents the contribution of the primary spectrometer, the medium dashed curve represents the $\delta d/d$ term, the long dashed curve represents the second term in Eqn. 2.1.10, and the smooth curve shows the total resolution of the spectrometer.

Optimization of the secondary spectrometer began with the desire to keep the first term in Eqn. 2.1.10 small compared to the second. This is achieved by minimizing the flight path uncertainty in Eqn. 2.1.6 and places a restriction on the maximum angle the analyzers can extend from the scattering plane. For perfect crystal analyzers, $\delta\theta_B$ in the second term of Eqn. 2.1.10 is dominated by the sample size in similar fashion to Eqn. 2.1.14. The curve in Fig. 5 was calculated for $\delta\theta_B = 0.3$ deg. For sample dimensions of 3 cm x 3 cm, this implies a sample-analyzer distance of ~2.5 m. The third term in Eqn. 2.1.10 is adjustable and depends on the thickness of the analyzer crystals and the radius to which they are curved. For ideal matching contributions to the resolution, $\delta d/d$ should be 3.5×10^{-4} for the Si (111) analyzers. Bending the crystals of appropriate thickness to a radius of 2.5 m brings the design close to the breaking limit for Si.

The inelastic resolution can also be calculated using the above equations and is shown in Fig. 6 for the Si (111) analyzers. Use of this side gives a greater dynamic range in ω than can be achieved with the Si (311) analyzers. The dynamic range for the Si (311) analyzers is limited by higher order Bragg reflections from the analyzers. These higher order reflections from the Si (111) analyzers are eliminated by a filter.

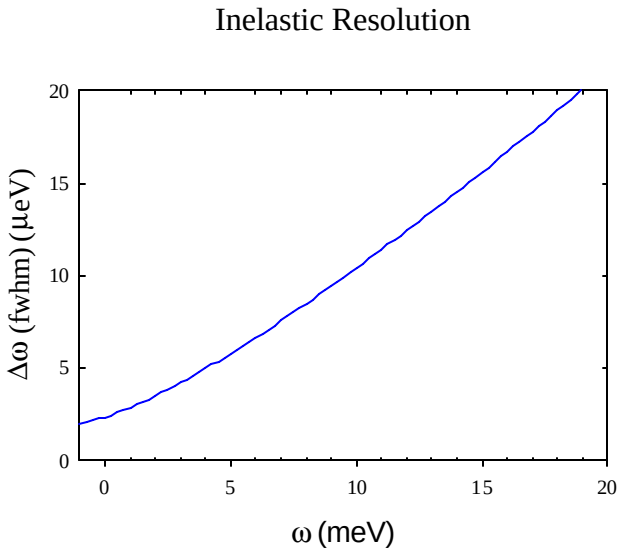

Figure 6. Inelastic resolution of the spectrometer when using the Si (111) analyzers.

Given the design requirements for high energy resolution using the Si (111) analyzers, the performance and design for a shorter wavelength (high-*Q*) option can be examined. With an 84 m incident flight path and the specified moderator, the primary spectrometer gives a contribution to the resolution function of 6.1 μeV for $\lambda = 3.273$ Å, the final neutron wavelength for the Si (311) analyzers. Resolution of the secondary spectrometer can be matched to this term using a $\delta d/d = 4 \times 10^{-4}$, with all dimensions remaining identical to those used for the Si (111) analyzers. Thus the two sides of the

secondary spectrometer are identical except for the type of crystal used to populate the analyzers. The total elastic resolution using the Si (311) analyzers is ~9 μeV.

2.3 Guide Optimization

Preliminary guide optimization was carried out by iteration of a Monte Carlo simulation. The guide begins at the leading edge of the shutter, 2.5 m from the moderator. Placing the guide another 1 m closer would result in a flux gain of 10%, but is much more complicated from an engineering standpoint. A curved guide was selected with radius chosen to give a critical wavelength of 2 Å for a supermirror guide with a critical angle twice that of natural nickel. This gives a radius of curvature of 4.3 km for a 10 cm wide guide. Line of sight from the moderator is reached with this design at a distance of 59 m and it is anticipated that substantial beam line shielding will have to extend to this distance. Optimization of the funnel in the horizontal direction resulted in a 5 m long $3\theta^{Ni}_c$ supermirror funnel that ends 30 cm from the sample with an exit dimension of 3 cm. The guide is 12 cm tall and ends in a 6 m long $3\theta^{Ni}_c$ supermirror funnel that also stops 30 cm from the sample with an exit dimension of 3 cm. Total guide gains were calculated at 1200 for λ = 6.2 Å and 400 for λ = 3.2 Å. Figure 7 shows the spatial distribution of neutrons at the sample position and the angular distribution of neutrons integrated over the 3 cm sample dimensions.

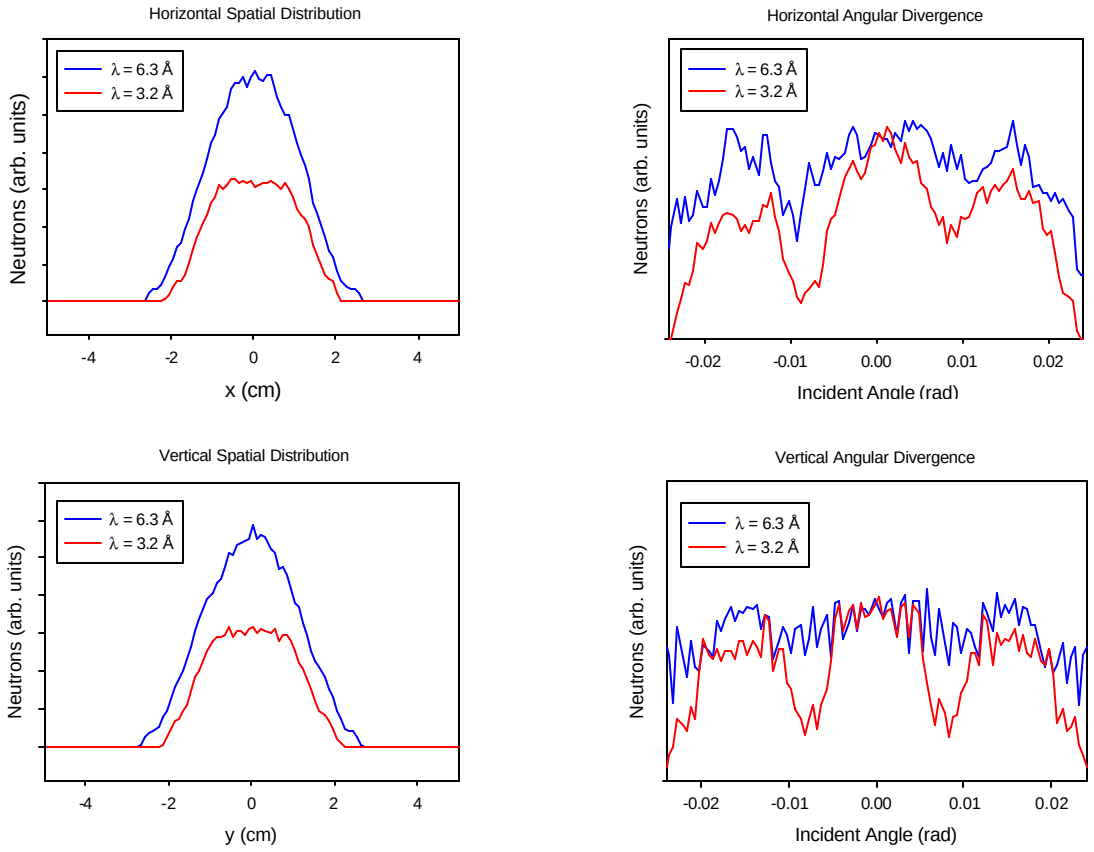

Figure 7. Distributions of neutrons at the sample position as determined from a Monte Carlo simulation. The lower curves in each plot are for λ = 3.2 Å, while the upper curves are for λ = 6.3 Å.

There are two general features that restrict the wavelength band of this spectrometer. For the case of the high energy resolution hemisphere using Si(111) analyzers, the wavelength band is limited by the repetition rate of the source. Higher order Bragg reflections from the analyzer crystals are removed by the filters located in front of the detectors. In this case the band width is given by the time required for the fastest neutrons from a given subsequent pulse to reach the sample simultaneously with the slowest neutrons from a previous pulse. Eliminating pulses can thus extend the wavelength band. If n is the number of intervening pulses eliminated, the wavelength band accepted by the spectrometer is given by

$$\Delta\lambda = \frac{(n+1)3955.4}{f\ L_i} \qquad 2.4.1$$

where f is the source frequency (60 hz) and L_i is the incident flight path length (m). Thus $\Delta\lambda$ = 0.785 Å if accepting every pulse from the source. This equation is also valid when using the diffraction capabilities of the instrument, except that L_i must be replaced by the total flight path length.

When using the Si(311) analyzers, the wavelength band is limited by higher order Bragg reflections from the analyzers. The next order reflection that is allowed is the Si(933) with a d-spacing of 0.546 Å, corresponding to a final neutron wavelength of $\lambda_{(933)}$ = 1.091 Å. Contamination free scattering occurs when the wavelength band is limited so that down-scattered neutrons reflected by the (311) reflection do not interfere with up-scattered neutrons reflected by the (933) reflection. This wavelength band is given by

$$\Delta\lambda = \frac{L_f}{L_i}\left(\lambda_{(311)} - \lambda_{(933)}\right) \qquad 2.4.2$$

With the specified flight paths, L_i = 84 m and L_f = 4.5 m, this corresponds to a bandwidth of 0.117 Å.

2.5 Chopper Timing and Operation

The bandwidth requirements given in Sec. 2.4 make placement of the bandwidth choppers critical, especially for operation of the Si (311) analyzers. Optimization of this system was done with a spreadsheet calculation that examined chopper transmissions and open times. In order to achieve a reasonable sweep time through the beam guide, one chopper must have a relatively large diameter in order to trim unwanted neutrons. This chopper should be as far from the source as practical. The chopper specified in Table III is partially open/closed for $\delta\lambda$ = 0.025 Å. In order to achieve clean operation using every pulse, three choppers are required for the Si (111) analyzers and an additional chopper is required for use of the Si (311) analyzers giving a total of 4 bandwidth choppers. Figures 8 – 10 show the chopper phasing and transmissions for three applications.

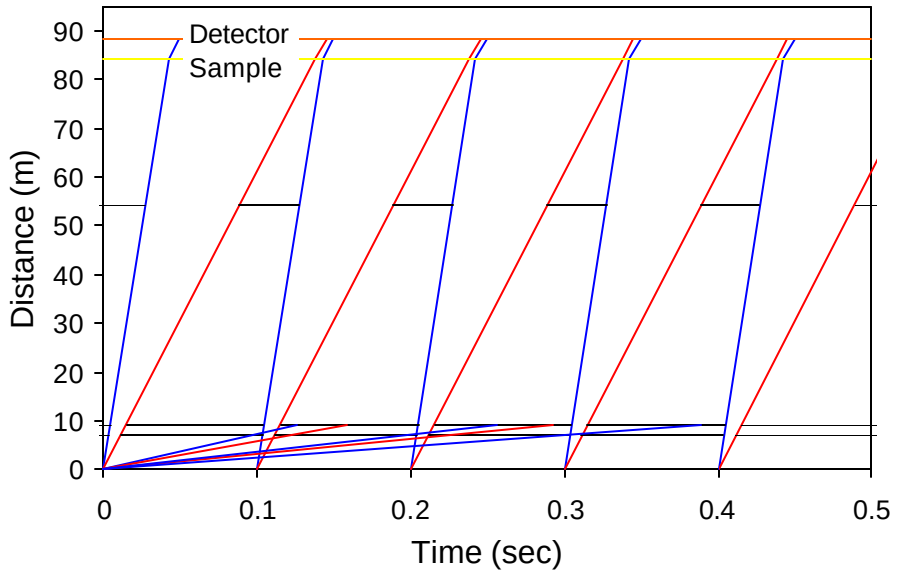

Figure 8. Timing diagram for using one pulse in 6 giving a wavelength band of 4.5 Å. This mode requires use of choppers 1-3 running at 10 hz. Full open/close of chopper 3 is achieved over a wavelength range of 1 Å. This is a possible operation mode when the diffraction detectors are to be used.

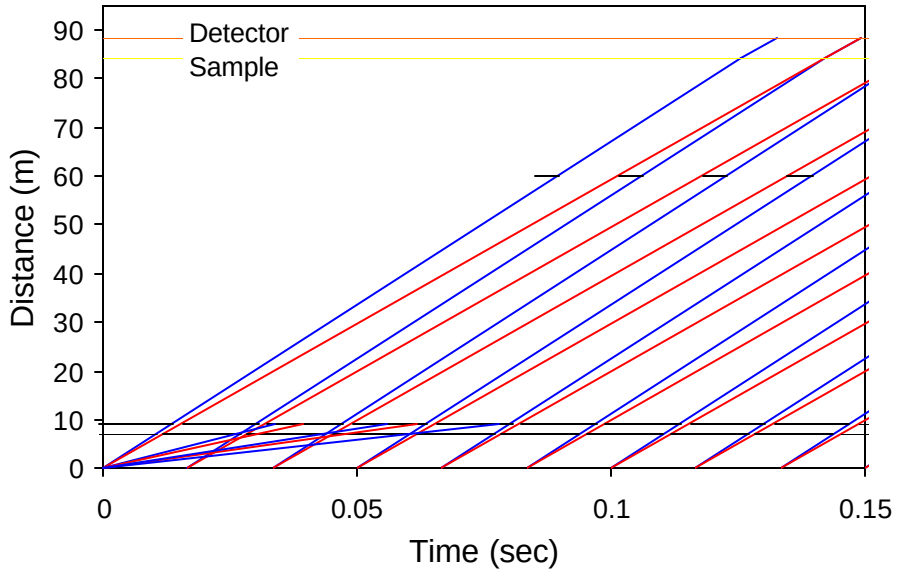

Figure 9. Timing diagram for using every pulse giving a wavelength band of 0.785 Å. This mode requires use of choppers 1,2 and 4 running at 60 hz. Full open/close of chopper 4 is achieved over a wavelength range of 0.025 Å. The bandwidth has been selected to illustrate the case of quasielastic scattering using the Si (111) analyzers.

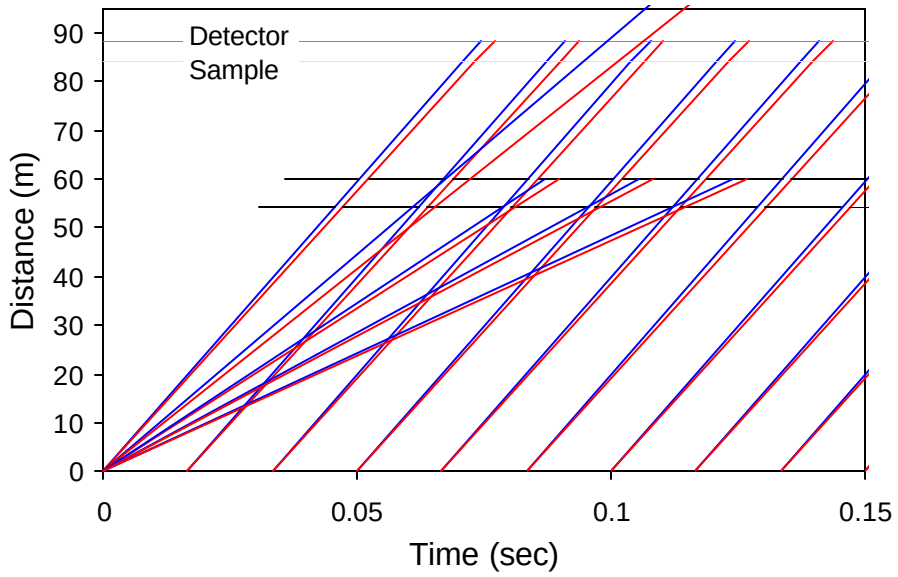

Figure 10. Timing diagram for using every pulse giving a wavelength band of 0.12 Å. This mode requires use of choppers 3 and 4 running at 60 hz. Full open/close of chopper 4 is achieved over a wavelength range of 0.025 Å. This is the mode that will be used when employing the Si (311) analyzers for quasielastic scattering. The band that comes through the second frame of the choppers can be separated at the detector by time of flight.

2.6 Analyzer Focussing and Detector Geometry

One of the most crucial aspects of this design is the location of the crystal analyzers and detectors relative to the sample location. In addition, it is required that the crystals be bent spherically (this is much more efficient at increasing $\delta d/d$ than other types of bending) and that the analyzers operate out of direct backscattering. Figure 11 is a sketch of the parameters used in the optimization of the analyzer/detector layout. The parameters that were optimized include, the detector placement (h_D and r_D), the detector tilt relative to the scattering plane normal (α), the radius of rotation for the analyzers, and the center of rotation for the analyzers. For the large analyzers, the detector and analyzer dimensions were then rotated about the scattering plane normal passing through the sample position. For the forward scattering analyzers, the detector and analyzer dimensions were rotated about the neutron beam line passing through the sample position. This surface is then slightly torroidal with one rotation axis (r_2) smaller than the other (r_1). (Note that r_2 varies slightly with position on the analyzer surface.) As a consequence the analyzer bending is not exactly spherical. A calculation of the contributions to the resolution resulted in the optimizations recorded in Table IV. It is important to note that the uncertainty in the final flight path has been averaged over the length of an individual detector tube. With position encoding along the length of individual detector tubes this term can be reduced much further. The lower analyzer and detector geometry are mirror reflections of the upper banks about the scattering plane.

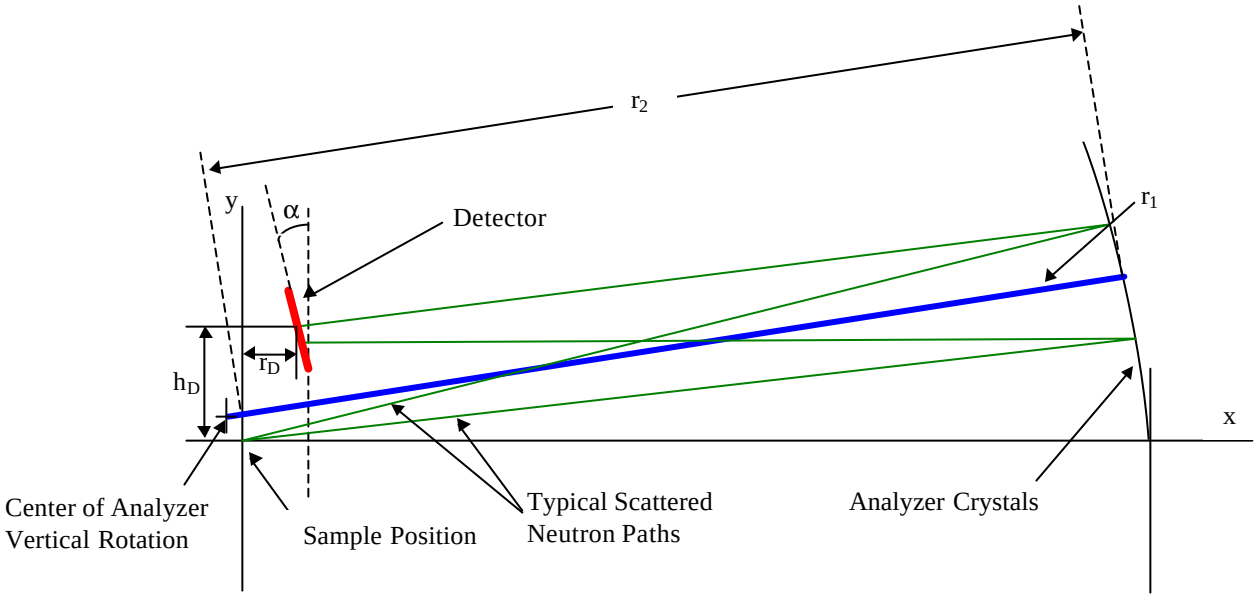

Figure 11. Geometry for analyzers and detectors. The blue line is r_1, one of the rotation axes of the analyzer crystals.

Table IV. Optimized parameters for the analyzer and detector geometry. The (x,y) coordinates of the center of rotation for the analyzers are given relative to the sample at (0,0).

	x (cm)	y (cm)	r_1 (cm)	r_2 (cm)	h_D (cm)	r_D (cm)	α (deg)
side analyzers	-0.61	8.70	250.0	249.4	20.0	31.0	11
forward analyzers	-2.11	8.47	250.0	247.85	35.0	42.5	8

3. Instrument Performance

3.1 Comparison to Existing Instruments

The instruments that can most readily be compared to this spectrometer in performance are backscattering spectrometers at reactor sources. In particular, the low-resolution mode of the newest ILL spectrometer, IN16, will be compared to the performance of the high-resolution side (Si (111) analyzers) and IN13 will be compared to the performance of the side using Si (311) analyzers. The time required to complete an experiment on the reactor instruments is dependent on the range of energy transfers covered. The relevant comparison to make for the primary spectrometers is the incident time-averaged flux on sample. The time averaged flux on sample for the SNS instrument is given by

$$F_{\mathrm{SNS}} = F'_{\mathrm{SNS}} \times D \qquad 3.1.1$$

where F'_{SNS} is the time averaged flux/μeV and D is the dynamic range of the measurement. Comparison between the secondary spectrometers is based on the ratio of solid angle intercepted and the $\delta d/d$ accepted by the analyzer. The ratio of time required for an SNS experiment to that of the relevant reactor instrument is given (for identical sample sizes) by

$$\frac{t_{\mathrm{SNS}}}{t_{\mathrm{Reactor}}} = \frac{F_{\mathrm{Reactor}}}{F_{\mathrm{SNS}}} \times \frac{A_{\mathrm{Reactor}}}{A_{\mathrm{SNS}}} \times \frac{\Omega_{\mathrm{Reactor}}}{\Omega_{\mathrm{SNS}}} \times \frac{\delta d/d_{\mathrm{Reactor}}}{\delta d/d_{\mathrm{SNS}}} \qquad 3.1.2$$

where F_{Reactor} is the time averaged flux on sample at the reactor, $\Omega_{\mathrm{Reactor}}$ and Ω_{SNS} are respectively the solid angle intercepted by the analyzer at the reactor and SNS, and the last term in Eqn. 3.1.2 represents the analyzer response. A_{Reactor} and A_{SNS} are respectively the sample dimensions at the reactor and SNS. Table V gives the relevant parameters of IN16 and IN13 while Table VI lists those for the SNS spectrometer. Note that F'_{SNS} has been determined from a Monte Carlo calculation of the moderator and assumes ideal guide performance. $\delta d/d$ for the reactor instrument has been calculated based on the performance of the spectrometer for the ideal case of matched resolutions. The remaining values are those published on the instrument web pages.

Table V. Parameters of IN16 and IN13 at the ILL.

	F (n cm^{-2} sec^{-1})	A (cm^2)	Ω (ster)	$\delta d/d$
IN16	1 x 10^5	12.0	1.8	~1.5 x 10^{-4}
IN13	2 x 10^4	12.25	1.26	~4 x 10^{-4}

Table VI. Parameters of the SNS spectrometer

Analyzers	*F'* (n cm^{-2} sec^{-1} μeV^{-1})	*A* (cm^2)	Ω (ster)	δd/d
Si (111)	8.4×10^4	9.0	1.3	$\sim 3.5 \times 10^{-4}$
Si (311)	1.65×10^4	9.0	1.2	$\sim 4 \times 10^{-4}$

Table VII makes the comparison between IN16 and this spectrometer using the Si (111) analyzers for a variety of dynamic ranges or types of measurements. A dynamic range of 1.4 μeV corresponds to a measurement of just the elastic intensity. Although the *Q*-ranges on these spectrometers are identical, it should be noted that IN16 was designed to give a factor of 2 better ω-resolution. The purpose of the table is to illustrate the effective duration of an experiment on either instrument assuming an energy resolution of 2 μeV is adequate (the *Q*-resolution and *Q*-range of the two instruments are identical). It should also be noted that the maximum dynamic range of the SNS instrument in the near elastic region is ±258 μeV a range that cannot be achieved with a reactor instrument even using the most sophisticated Doppler drive monochromators. The maximum range achieved on IN16 is ±15 μeV. Another advantage of the SNS spectrometer is its ability to perform inelastic measurements to energy transfers of 18 meV with extremely good energy resolution.

Table VII. A comparison of experiment duration between IN16 and the SNS spectrometer using Si(111) analyzers.

D (μeV)	$t_{SNS}/t_{Reactor}$
1.4	0.67
10	0.09
30	0.03
100	0.009

Table VIII makes the comparison between IN13 and this spectrometer using the Si (311) analyzers. A dynamic range of 6.9 μeV corresponds to a measurement of just the elastic intensity. The *Q*-range and *Q*-resolution is similar for these spectrometers although IN13 has a maximum *Q* of 5.5 $Å^{-1}$ to be compared with a maximum *Q* of 3.9 $Å^{-1}$ for the SNS spectrometer. The energy resolutions are nearly identical. The range of energy transfers that can be achieved with IN13 is –125 μeV to 300 μeV, comparable to the performance of the SNS spectrometer.

Table VIII. A comparison of experiment duration between IN13 and the SNS spectrometer using Si(311) analyzers.

D (μeV)	$t_{SNS}/t_{Reactor}$
6.9	0.25
100	0.017
200	0.0087
425	0.0043

In summary, for measurements of only the elastic intensity where the reactor instruments in their point-by-point measurement are most effective, the SNS spectrometer will perform comparable to IN16 and ~4 times faster than IN13. For experiments that use the entire dynamic range of the reactor spectrometers (30 μeV for IN16, 425 μeV for IN13) the SNS instrument will take data 30 times faster than IN16 and 230 times faster than IN13. For experiments that use the entire dynamic range available with the most advanced Doppler shifting monochromators (100 μeV), the SNS spectrometer will be 100 times faster.

3.2 Detector Performance and Estimated Count Rates

The peak count rate is expected to occur at the elastic peak for a strongly scattering sample. This situation arises in the case of an inelastic measurement where multiple scattering in the sample is of limited concern and the total sample scattering may approach 30% of the incident beam flux. Assuming that the majority of these neutrons are scattered elastically, the number of neutrons scattered by the sample into the elastic peak is given by

$$N_S = F \times s \times w_R \times 0.3 \qquad 3.2.1$$

where F is the expected flux on sample, s is the sample size, and w_R is the resolution width of the primary spectrometer. For the high-resolution spectrometer, F = 8.4x10^4 n/cm^2-sec-μeV (2 MWatt SNS, guide gain of 1200), s is 9 cm^2, and w_R is 1.4 μeV, making N_S = 3.2x10^5 n/sec.

The analyzer segments located from 20 deg to 160 deg in scattering angle intercept 0.6 ster of solid angle each (two on each side of the spectrometer, located above and below the scattering plane). Each analyzer segment illuminates its associated detector bank in a nearly uniform fashion. Each analyzer intercepts 0.6/4π (0.048) of the total solid angle and focuses these neutrons back onto the detector bank, which has a surface area of 1760 cm^2. The total time averaged flux onto a single detector bank, F_D, is given by

$$\begin{aligned} F_D &= 0.048 \times N_S \,/1760\,\mathrm{cm}^2 \\ &= 8.7 \text{ n/cm}^2\text{-sec} \end{aligned} \qquad 3.2.2$$

The peak count rate is also of importance and may be calculated from

$$P = 2 \times F_D \times \frac{1}{f} \times \frac{1}{t_R} \qquad 3.2.3$$

where f is the source frequency (60 Hz) and t_R is the time band over which the elastic peak is measured. The factor of 2 comes from estimating the peak count rate rather than the average count rate over this time bin and is correct for a triangular shaped resolution function. At a moderator-detector flight path of 88.5 m, ±1.1 μeV band of neutrons is spread into a time width of t_R =74 μsec. P is then 3.9x10^3 n/cm^2-sec. The peak count rate averaged over all the detectors in a single bank is 6.9 x 10^6 n/sec.

It is also of interest to estimate the time required to obtain counts in the peak channel of the elastic peak for a typical quasielastic scattering measurement where the sample transmission is typically 0.9. Let P_T be the desired number of counts, then the time t required to make this measurement can be estimated from

$$t = P_T \times \frac{1}{F_D} \times \frac{1}{A_D} \times \frac{N_R}{2} \qquad 3.2.4$$

where A_D = 70.4 cm^2 is the detector area that gets summed into a single Q-point. For a 10% scattering sample F_D = 2.9 n/cm^2-sec, and N_R is the number of time bins across the elastic peak into which counts are stored (a typical value is 20, the factor of 2 is correct if the resolution shape were triangular). As an example, the time required to measure P_T = 4000 counts in this time bin for a single Q is approximately 3 minutes. Recall though that there are two identical analyzer/detector banks on each side of the instrument, so this number of counts should be obtained in less than 2 minutes. A similar analysis done for the IRIS instrument at ISIS resulted in an overestimate of 70% for the count rates at the detectors. At least part of this discrepancy can be accounted for by not including the effects of windows or imperfect guides. The numbers given above should represent an upper bound on the detector requirements.

4.0 Research and Development Efforts

The performance of the analyzer crystals is crucial to the operation of this spectrometer. In order to obtain the desired $\delta d/d$ for a bending radius of 2.50 m, the Si (111) crystals must be of a thickness that will take the crystals close to the breaking limit. In addition, there is little information available for bent Si (311) crystals. The following is a list of questions or topics that need to be investigated about the analyzer crystals:

1. Breaking limit of Si (111) as both thickness and bending radius are varied near the operating conditions of this spectrometer.

2. $\delta d/d$ as a function of Si (111) thickness and bending radius.

3. Breaking limit of Si (311) as both thickness and bending radius are varied near the operating conditions of this spectrometer.

4. $\delta d/d$ as a function of Si (311) thickness and bending radius.

5. The effectiveness of various glues in holding crystals of the appropriate thickness to an aluminum surface.

6. What is the expected thermal diffuse scattering and how will it contribute to the background levels of the instrument?

Another critical component is the chopper system. The system must be extremely flexible and its operating parameters must be very user friendly and easy to change. In addition, the Si (311) analyzers can only use a very narrow bandwidth. Although the current design takes advantage of the flight path and places a chopper at 60 m, its open/close time corresponds to a $\Delta\lambda$ of 0.025 Å. This is a reasonable fraction of the desired bandwidth, 0.12 Å. It is desirable to have a chopper that performed even better than specified. Alternatively, or in combination, one can think of compressing and than expanding the neutron beam, giving a narrower path for the chopper to pass through. The available technology needs to be examined in order to improve this parameter.